Aeromagnetic Surveys over the Yamato Mountains and the Yamato Meteorite Ice Field, East Antarctica

Kazuo SHIBUYA*, Akiko TANAKA** and Mitsuru MANABE***

東南極のやまと山脈およびいん石氷原上における航空磁気測量

渋谷和雄*・田中晶子**・真部允宏***

要旨: やまと山脈およびいん石氷原の地域で, 1975 年および 1980 年に航空磁気測量を行った. これらの観測結果を解析して, 基盤岩の地質, 帯磁率, 地形などとの関連性を検討した結果, 観測された地磁気異常分布は, 氷床下の基盤の地形と最も関係が深いと解釈しうることがわかった.

Abstract: Aeromagnetic surveys were conducted in the Yamato Mountains and the Meteorite Ice Field region in 1975 and 1980, using Cessna A185F and Pilatus Porter PC-6 aircrafts respectively. Distribution of geomagnetic anomaly in this area obtained from those surveys is thought to be correlated mostly with the subglacial topography other than types or magnetic susceptibility of bedrocks.

1. Introduction

According to SEASAT configuration of the Antarctic ice sheet in the sector 30°–80°E (Fig. 6 in SHIBUYA *et al.*, 1986), a long ridge can be traced along 40°E meridian line, and the Yamato Mountains are located close to the western side of the above ridge. They consist of 7 outcrop areas which are named A to G Gun (A to G Groups) and are extending from south to north as illustrated by solid curves in Fig. 1. The Yamato Mountains are also situated near the eastern end of the sub-ice Sør Rondane Mountains extending nearly parallel to the Antarctic Sea coast. The dam effect of the Yamato Mountains for the upstream ice sheet results in the up-welling of the ice flow stream lines, which in turn results in the large bare ice area characterized by the snow surface ablation and concentration of meteorites (NAGATA, 1978). The moraine fields which cover the ice surface near the mountains (dotted curves in Fig. 1) are considered to have been brought from the bottom of the ice sheet by upwelling.

In December 1975, the 16th Japanese Antarctic Research Expedition (JARE-16) made an aeromagentic survey flight for the first time over the Yamato Mountains using Cessna A185F equipped with a proton magnetometer, which is called arbitrarily Flight Y0 here (GEOGRAPHICAL SURVEY INSTITUTE, 1986). Five years after the above survey,

* 国立極地研究所. National Institute of Polar Research, 9-10, Kaga 1-chome, Itabashi-ku, Tokyo 173.
** 日本大学文理学部応用地学教室. Department of Applied Earth Science, College of Humanities and Sciences, Nihon University, 25-40, Sakura-jousui 3-chome, Setagaya-ku, Tokyo 156.
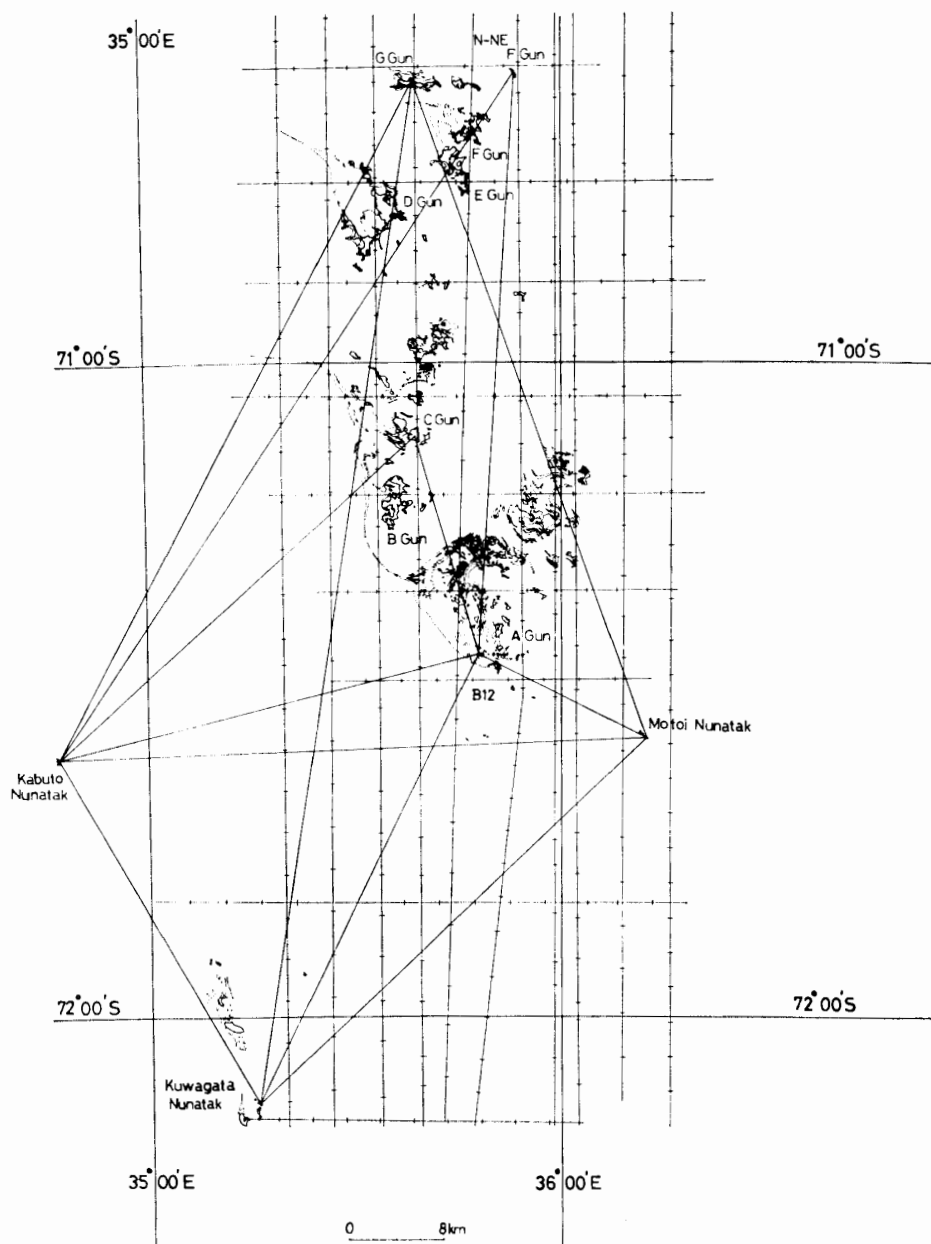*** 国土地理院. Geographical Survey Institute, 1, Kitazato, Yatabe-machi, Tsukuba-gun, Ibaraki 305.

Fig. 1. *The Yamato Mountains and the survey profiles of Flight Y0 and Flight Y1. Solid curves indicate outcrop areas and dotted curves indicate moraine fields, respectively.*

JARE-21 made another two flights (Flights Y1 and Y2) using Pilatus Porter PC-6 equipped with the M-123 (Barringer Co., Ltd.) proton precession magnetometer. Since the short-period time variation of geomagnetic fields during Flight Y2 (400 nT change in 4 h; see SHIBUYA, 1986) is too large for correction, the obtained total intensity data are not used for further analysis. Superposition of survey lines of Flights Y0 and Y1 still gives appropriate coverage over the Yamato Mountains, and the reduced geomagnetic anomaly profile of each flight may be integrated with a certain allowable contouring criterion after several correction procedures.

2.   Survey Flights and Data Analyses

2.1.   Survey flight

Figure 1 illustrates survey profiles of Flights Y0 and Y1. Two sets of parallel lines indicate flight courses C1–C20 of Flight Y0 in 1975 (JARE-16) and the total intensity data with every 2–5 km distance were read to 10 nT resolution from the display of the magnetometer. Geographical coordinates at the reading point were estimated from the aerial photographs (GEOGRAPHICAL SURVEY INSTITUTE, 1986).

Trigonometric survey lines indicate segments of Flight Y1 in 1980 (JARE-21) and the log is edited in Table 1 from the JARE Data Reports. The flight height was controlled at 10000 ft above sea level and the total intensity data were digitally recorded on a cassette tape with every 1.2 s interval (~60 m distance) to 1 nT resolution (SHIBUYA, 1986).

Geographical coordinates to each total intensity data in Flight Y1 were assigned by the method of proportional distribution using the successive departure and arrival times of flight for each successive control point in Table 1 and the number of data points in each flight segment.   From columns 8 and 9 of Table 1, the interval aircraft speed against ground for each flight segment can be as illustrated as in Fig. 2 taking the course direction as a parameter, which is consistent with almost uniform wind speed of 30–40 kn, 80°–100° wind direction and the controlled 100 kn flight speed of PC-6 against air during the survey.

Since the survey methods and the data acquisition system are similar to those in the previous analyses for the Shirase Glacier area (SHIBUYA and TANAKA, 1983) and for the moraine field to the north of Mizuho Station (SHIBUYA, 1985), their detailed
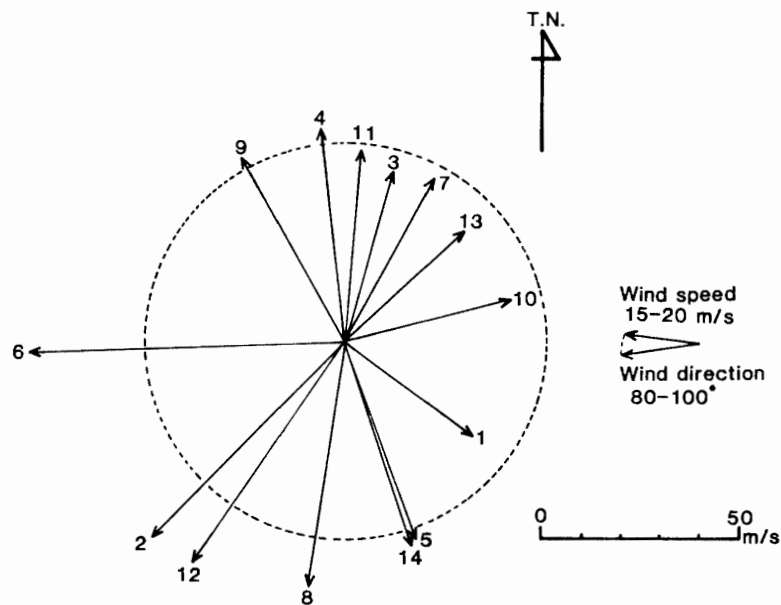

Fig. 2.   *Superposition of interval velocity vector of aircraft against ground. Number at the arrow corresponds to each flight segment number (column 1), direction of the arrow to course direction (column 8) and the length of the arrow to interval speed (column 9), respectively in Table 1.*

Table 1. *Log of Flight Y1, edited from* SHIBUYA *(1986).*

Flight Y1 (1955–2355 LT, December 12, 1980)

Segment number	Control point	Departure time	Distance (km)	Estimate time of elapse	Estimate time of arrival	Actual time of arrival	Course direction (degree)*	Interval speed (m/s)
	B12	$20^h13^m30^s$						
1			15.4	5^m10^s	$20^h18^m40^s$	$20^h20^m00^s$	121	39.5
	Motoi Nunatak	20 20 00						
2			45.6	15 30	20 35 30	20 31 00	224	69.1
	Kuwagata Nunatak	20 31 00						
3			43.5	14 50	20 45 50	20 47 00	16	45.3
	B12	20 47 00						
4			49.4	16 50	21 03 50	21 02 00	354	54.9
	G Gun	21 02 00						
5			59.3	19 00	21 21 00	21 20 30	160	53.4
	Motoi Nnuatak	21 20 30						
6			49.6	17 00	21 37 30	21 31 00	268	78.7
	Kabuto Nunatak	21 31 00						
7			66.1	22 30	21 53 30	21 54 00	28	47.9
	G Gun	21 54 00						
8			89.5	30 30	22 24 30	22 18 00	189	62.2
	Kuwagata Nunatak	22 18 00						
9			34.3	11 40	22 29 40	22 28 30	331	54.4
	Kabuto Nunatak	22 28 30						
10			37.4	12 50	22 41 20	22 43 00	75	43.0
	B12	22 43 00						
11			50.0	17 00	23 00 00	23 00 00	4	49.0
	N. NE F Gun	23 00 00						
12			71.7	24 30	23 24 30	23 17 30	214	68.3
	Kabuto Nunatak	23 17 30						
13			41.7	14 10	23 31 40	23 34 00	47	42.1
	C Gun	23 34 00						
14			19.6	6 40	23 40 40	23 40 00	163	54.4
	B12	23 40 00 (arrival)						

* Measured from geographic north.

explanation is not mentioned here.

2.2. Reduction to geomagnetic anomaly

Figure 3 shows the reduction procedure from the observed total intensity profile $F_{observed}$ (Fig. 3a) to the geomagnetic anomaly profile $F_{anomaly}$ (Fig. 3d) by subtracting the International Geomagnetic Reference Field F_{IGRF} over the profile concerned (Fig. 3b) and the short-period time variation by the earth's external field $F_{diurnal}$ (Fig. 3c). Since the direction of magnetic course of each flight segment has mostly only small offset against the direction of the isomagnetics, the short-wavelength variation of $F_{observed}$ (10–50 km) is considered to be correlated with the local subglacial topographic and geological structures. $F_{diurnal}$ during the survey flight, however, is rather large (-100 to 100 nT) with the change-period of 5 to 20 min especially corresponding to the profile portions between Kabuto Nunatak and Motoi Nunatak, and between Kabuto Nunatak and G Gun (Fig. 3c), which inevitably overlaps the 20–50 km spatial change of the geological structure and may introduce artificial geomagnetic anomaly highs and lows.

By the elapse time of 5 years between Flights Y0 and Y1, the decrease of the intensity of the main geomagnetic field by a secular variation attained to about 700 nT (see Fig. 4 in SHIBUYA and TANAKA, 1983). The reduced geomagnetic anomaly for Flight Y0 by the similar procedure thus may have a constant offset against that of
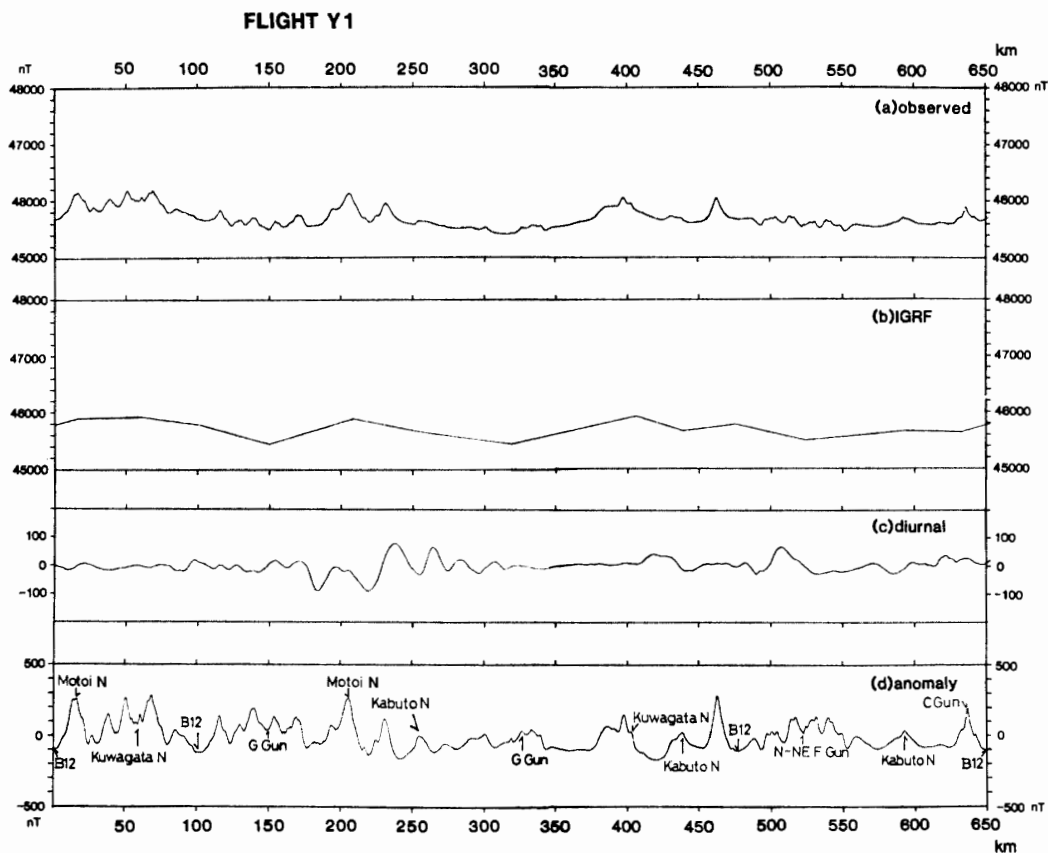

Fig. 3.   Reduction of the observed total intensity data to the geomagnetic anomaly for Flight Y1.   For details, see text.

Flight Y1 which resulted from the uncertainty in the change of the International Geomagnetic Reference Field.   In order to minimize the overall discrepancy between the two geomagnetic anomaly values, their difference at the 70 crossover points of the profiles were averaged to obtain the correction term to the anomaly of Flight Y1. After subtracting the resultant 32 nT offset from the anomalies of Flight Y0, the anomaly values were adjusted to those of Flight Y1.

2.3. Contouring of geomagnetic anomalies

The combined geomagnetic anomaly values along the flight profile are plotted onto a 1 : 200000 topographic sheet of the Yamato Meteorite Ice Field with every
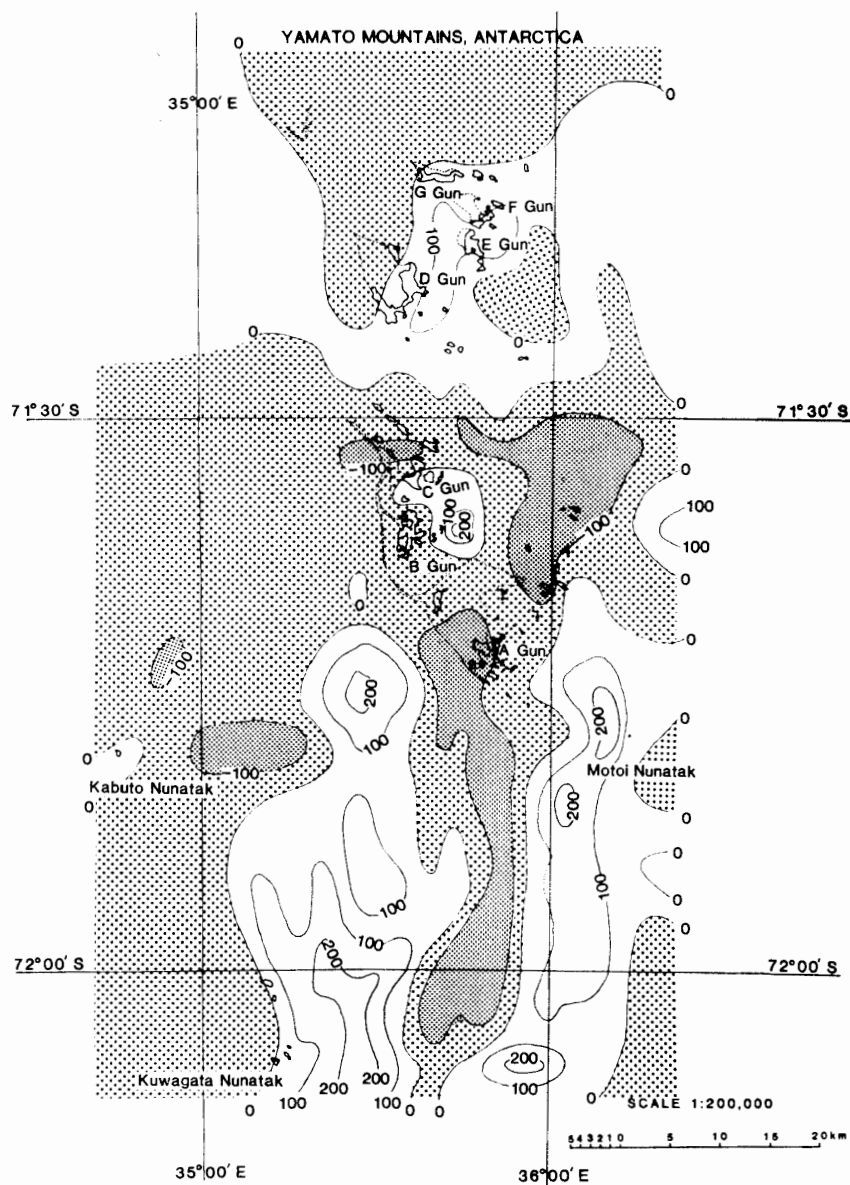

Fig. 4. Geomagnetic anomalies over the Yamato Mountains and the Yamato Meteorite Ice Field. Sheded portion corresponds to areas of negative value. Contouring interval is 100 nT.

0.5 km distance. The anomaly values within a rectangle of 4 by 4 km are averaged in order to supress short-wavelength noise around the crossover points. The anomaly values are then grouped into several ranges of 50 nT interval. There still remain several portions of discordant anomaly trends. Try and error adjustment by eye for the above preliminary anomaly distribution finally resulted in the geomagnetic anomalies of 100 nT contouring interval as shown in Fig. 4.

In Fig. 4, the obtained geomagnetic anomalies range mostly from -200 to 300 nT. The shaded region is characterized by negative and lower anomalies for thicker-shaded areas. The Yamato Mountains geomagnetic anomalies can qualitatively be divided by a boundary at around $71°30'S$. The northern part of the boundary is characterized by a gentle pattern with a positive high covering the outcrop areas of D, E, F and G Gun. The southern part of the boundary is on an average in the range of -100 to 0 nT, and an east-west undulation of the south-to-north elongated anomalies of ± 200 nT amplitude overlaps that average filed. The valley of -100 to -200 nT anomaly lows is situated along $35°50'E$, which is accompanied by two parallel anomaly highs of 100 to 200 nT. The predominant wavelength of the east-west undulation is 20–25 km. The northern portion of the above elongated pattern is shifted eastward from around $71°40'S$ and the anomaly becomes less pronounced continuing to the gentle northern part of the boundary. It is noted that A Gun has anomaly lows of -100 to -200 nT, though the other outcrop areas are mainly characterized by positive anomalies.

3. Discussion

According to SHIRAISHI et al. (1982), the basement of the Yamato Mountains consists of high grade metamorphic, syenitic and granitic rocks. From petrologic observations, SHIRAISHI et al. (1982) subdivided metamorphic rocks into two-fold regions: older granulite-facies rocks and younger amphibolite-facies rocks. ASAMI and SHIRAISHI (1985) estimate that the maximum metamorphic temperature of the older granulite-facies rocks is about $750°C$ and the pressure is below 6 Kb. As compared with the P-T condition of up to $850°C$ and 10 Kb (MOTOYOSHI et al., 1985) of the granulite-facies metamorphism of the Lützow-Holm Complex in the Prince Olav Coast to the Lützow-Holmbukta region, the former Yamato–Belgica Complex of 700 Ma event (SHIBATA et al., 1985) is considered to have been formed at a higher crustal level. The younger amphibolite-facies metamorphism is interpreted as corresponding to the 500 Ma intrusion of granite and pegmatite (ASAMI and SHIRAISHI, 1983; SHIBATA et al., 1985) which is widely known in East Antarctica.

In order to see the correlation between the magnetic properties of rocks and the geomagnetic anomalies, magnetic susceptibility of the sample rocks from various localities is measured by the Bison susceptibility meter. Table 2 summarizes the results for 22 samples, where sample number is after each geology party of JARE. The obtained magnetic susceptibility has no systematic correlation with the areal or petro-graphical distribution, and the value ranges from 1.0×10^{-7} to 2.5×10^{-5} emu/g; which is considered typical for ilmenite-enriched metamorphic rocks. For a brief summary, the order of magnitude of the obtained susceptibility is shown in Fig. 5 by different size of an open circle with the locality of the sample.

Table 2. *Summary of the obtained magnetic susceptibility.*

Sample number	Locality	Rock name	Density (g/cm^3)	Magnetic susceptibility (emu/g)
73120606	F Gun	K-feldsper-porphyrite, clinopyroxene biotite	2.54	2.87×10^{-6}
75120703	E Gun	Clinopyroxene biotite gneiss	2.36	1.31×10^{-6}
75120701	E Gun	Clinopyroxene gneiss	2.60	8.9×10^{-7}
75121902	D Gun	Two-pyroxene biotite gneiss	2.65	2.16×10^{-5}
73120712	D Gun	K-feldspathic biotite granitic gneiss	3.00	3.9×10^{-7}
75120501	N.W.C. Gun	K-feldspathic biotite granitic gneiss	2.38	2.09×10^{-6}
75121001	C Gun	Clinopyroxene syenite	2.54	1.308×10^{-5}
75121006	C Gun	Clinopyroxene syenite	2.48	2.95×10^{-6}
Y80B26	B Gun	Feldspathic biotite granitic gneiss	2.32	2.504×10^{-5}
Y80B501	B Gun	Biotite amphibolite with K-feldspathic granite	2.02	1.123×10^{-5}
75122702	A Gun	Clinopyroxene syenite gneiss	2.56	1.0×10^{-7}
75122707	A Gun	Clinopyroxene biotite granite	3.00	2.0×10^{-7}
75122802	A Gun	Two-pyroxene biotite granitic gneiss	2.45	1.2×10^{-7}
73121402	Kabuto Nunatak	Hornblende biotite gneiss	2.61	1.4×10^{-7}
73121407	Kabuto Nunatak	Melano-hornblende biotite gneiss with aplite	2.65	4.7×10^{-7}
73121606	Kurakake Nanatak	K-feldspathic biotite granitic gneiss	2.42	2.49×10^{-6}
73121607	Kurakake Nunatak	Biotite granitic gneiss	2.60	1.323×10^{-5}
73121608	Kurakake Nunatak	Melano biotite gneiss	2.53	1.68×10^{-6}
73121609	Kurakake Nunatak	Quartz feldspathic gneiss	2.49	9.39×10^{-6}
73121709	Kuwagata Nunatak	Biotite gneiss with aplite	2.68	1.648×10^{-5}
73121704	Kuwagata Nunatak	Amphibolite with aplite	2.60	5.45×10^{-6}
73A002	Touchaku Rock	K-feldsper porphyrite, biotite granitic gneiss	2.46	1.034×10^{-5}

The variation of short-wavelength intensity of the regional crust is believed to be mostly related with the distribution of magnetite-enriched rocks. The retrograde metamorphism of the Yamato Mountains (Asami and Shiraishi, 1985) is not associated with the condensation of magnetite-enriched rocks considering the ground data in Table 2 or Fig. 5. The geomagnetic anomaly pattern in Fig. 4 then would be related mainly with the subglacial geomorphological structure of the region concerned.

According to Yoshida (1983), the Yamato Mountains had been completely covered by the ice sheet at its maximum expansion. There are three stagnant stages during the lowering of the ice sheet surface, named Yamato, Fukushima and Mete-
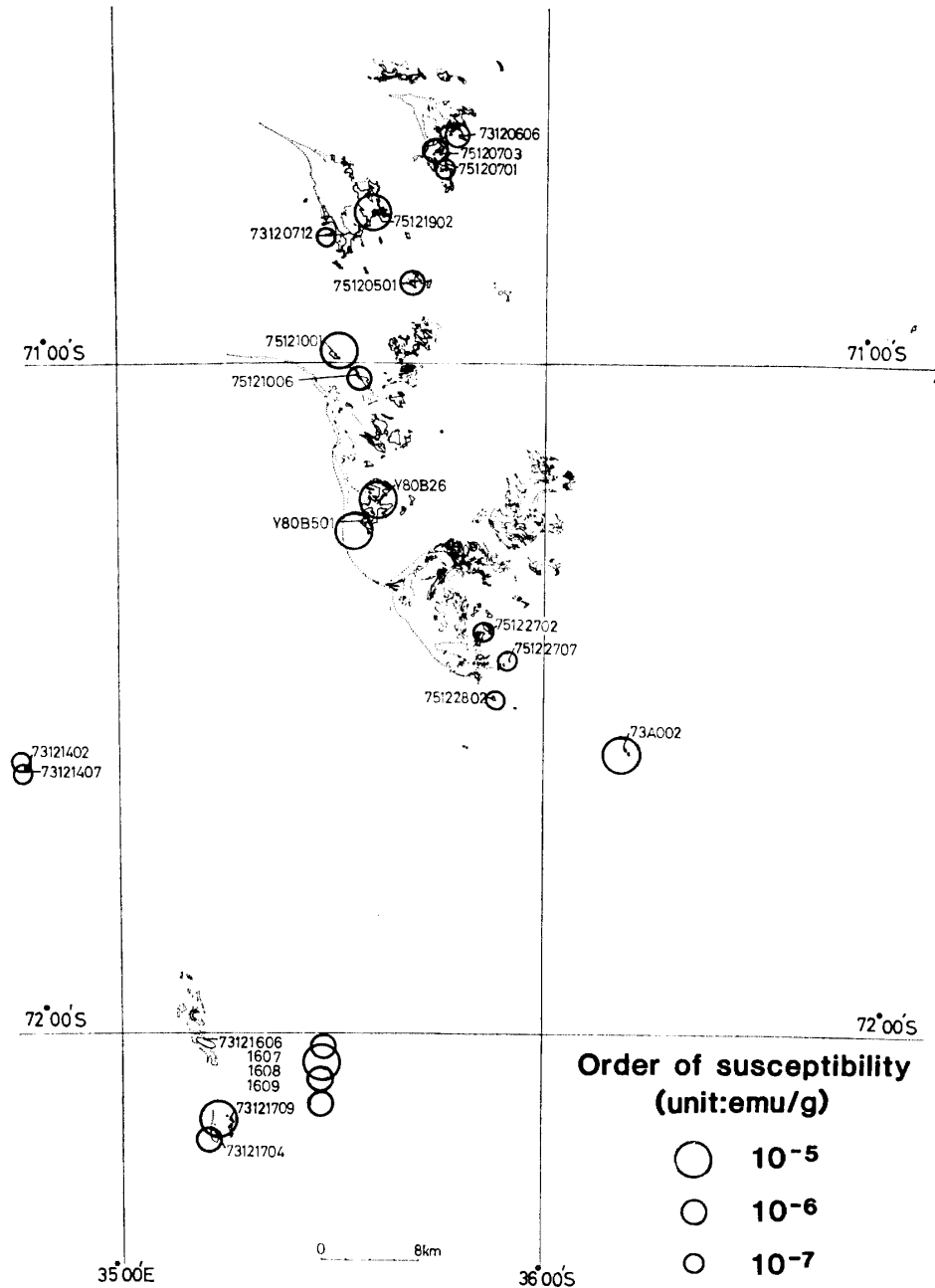
Fig. 5. *Locality of the sample rocks for magnetic susceptibility measurements.*
Sample name corresponds to that in Table 1.   The order of magnitude
of the obtained susceptibility is indicated by different size of an open
circle.

orite Glacial Stages. YOSHIDA (1985) indicates that the last ice retreat took place before 30 Ka age based on the degree of weathering. As for the past flow direction of the ice sheet, YOKOYAMA (1976) examined glacial striae at Kurakake and Kuwagata Nunataks (see Fig. 1) and indicates N30°W–N55°W direction. If the east-west undulation of the geomagnetic anomaly highs and a low in Fig. 4 would correspond to ridges and a valley of the bedrock topography, it is noted that the direction of the

above glacial striae has about 45° counterclockwise offset against the above south-to-north elongation (0°) of the geomagnetic anomalies.

The airborne radio echo sounding over the region concerned is progressing in the 1986–1987 summer season by JARE-27.   Interpretation of the geomagnetic anomalies together with the ice thickness distribution and gravity anomaly data would elucidate detailed subglacial and geophysical structure of the Yamato Meteorite Ice Field.

Acknowledgments

References

ASAMI, M. and SHIRAISHI, K. (1985): Retrograde metamorphism in the Yamato Mountains, East Antarctica.   Mem. Natl Inst. Polar Res., Spec. Issue, 37, 147–163.

GEOGRAPHICAL SURVEY INSTITUTE (1986): Outline of aeromagnetic surveys, 1967–1975, Antarctica (Kôkû jiki sokuryô gaikyô).   Collected Data of Gravimetric and Geomagnetic Surveys in Antarctica (Nankyoku Chiiki, Jûryoku·Chijiki Sokuryô Deta Shûroku), 57–171.

MOTOYOSHI, Y., MATSUBARA, S., MATSUEDA, H. and MATSUMOTO, Y. (1985):   Garnet-sillimanite gneisses from the Lützow-Holm Bay region, East Antarctica.   Mem. Natl. Inst. Polar Res., Spec. Issue, 37, 82–94.

NAGATA, T. (1978): A possible mechanism of concentration of meteorites within the Meteorite Ice Field in Antarctica.   Mem. Natl Inst. Polar Res., Spec. Issue, 8, 70–92.

SHIBATA, K., YANAI, K. and SHIRAISHI, K. (1985): Rb-Sr mineral isochron ages of metamorphic rocks around Syowa Station and from the Yamato Mountains, East Antarctica.   Mem. Natl Inst. Polar Res., Spec. Issue, 37, 164–171.

SHIBUYA, K. (1985): Geomagnetic anomalies over the moraine field to the north of Mizuho Station, East Antarctica.   Mem. Natl Inst. Polar Res., Spec. Issue, 37, 1–12.

SHIBUYA, K. (1986): Aeromagnetic survey around Syowa Station, Antarctica: (3) Flights No. 14–Y2 by JARE-21.   JARE Data Rep., 119, (Earth Sci. 3), 1–86.

SHIBUYA, K. and TANAKA, Y. (1983): An aeromagnetic survey over the Shirase Glacier.   Mem. Natl Inst. Polar Res., Spec. Issue, 28, 1–17.

SHIBUYA, K., KAJIKAWA, Y. and SEGAWA, J. (1986): Surface configuration of the Antarctic ice sheet in the sector 30°E–80°E using SEASAT altimetry data.   Mem. Natl Inst. Polar Res., Spec. Issue, 43, 1–12.

SHIRAISHI, K., ASAMI, M. and OHTA, Y. (1982): Plutonic and metamorphic rocks of Massif-A in the Yamato Mountains, East Antarctica.   Mem. Natl Inst. Polar Res., Spec. Issue, 21, 21–31.

YOKOYAMA, K. (1976): Geomorphological and glaciological survey of the Minami-Yamato Nunataks and the Kabuto Nunatak, East Antarctica.   Nankyoku Shiryô (Antarct. Rec.), 56, 14–19.

YOSHIDA, Y. (1983): Physiography of the Prince Olav and the Prince Harald Coasts, East Antarctica.   Mem. Natl Inst. Polar Res., Ser. C (Earth Sci.), 13, 83 p.

YOSHIDA, Y. (1985): A note on the ice sheet fluctuations and problems of Cenozoic studies in Antarctica.   Mem. Natl Inst. Polar Res., Spec. Issue, 37, 187–200.